Surface tension of magnetized quark matter

André F. Garcia and Marcus Benghi Pinto*
Departamento de Física, Universidade Federal de Santa Catarina, 88040-900 Florianópolis, Santa Catarina, Brazil
(Received 18 June 2013; revised manuscript received 6 August 2013; published 22 August 2013)

The surface tension of quark matter plays a crucial role for the possibility of quark matter nucleation during the formation of compact stellar objects and also for the existence of a mixed phase within hybrid stars. However, despite its importance, this quantity does not have a well-established numerical value. Some early estimates have predicted that, at zero temperature, the value falls within the wide range $\gamma_0 \approx 10$–$300\,\mathrm{MeV/fm^2}$ but, very recently, different model applications have reduced these numerical values to fall within the range $\gamma_0 \approx 5$–$30\,\mathrm{MeV/fm^2}$, which would favor the phase conversion process as well as the appearance of a mixed phase in hybrid stars. In magnetars one should also account for the presence of very high magnetic fields which may reach up to about $eB \approx 3$–$30\,m_\pi^2$ ($B \approx 10^{19}$–$10^{20}\,G$) at the core of the star so it may also be important to analyze how the presence of a magnetic field affects the surface tension. With this aim we here consider magnetized two-flavor quark matter, described by the Nambu–Jona-Lasinio model. We show that although the surface tension oscillates around its $B = 0$ value, when $0 < eB \lesssim 10m_\pi^2$, it only reaches values which are still relatively small. For $eB \approx 5.5m_\pi^2$ the $B = 0$ surface tension value drops by about 30% while for $eB \gtrsim 10m_\pi^2$ it quickly raises with the field intensity so the phase conversion and the presence of a mixed phase should be suppressed if extremely high fields are present. We also investigate how thermal effects influence the surface tension for magnetized quark matter.

DOI: 10.1103/PhysRevC.88.025207 PACS number(s): 21.65.Qr, 11.10.Wx, 12.39.Ki, 26.60.Kp

I. INTRODUCTION

The understanding of compact stars requires the study of strongly interacting matter at low temperatures and high chemical potentials. However, this portion of the QCD phase diagram cannot be addressed by current lattice-QCD methods so studies of this phase region must rely on less fundamental models. Most investigations suggest that there is a first-order chiral phase transition which, for $T \approx 0$, sets in at baryon densities several times that of the nuclear saturation density, $\rho_0 \approx 0.17\ \mathrm{fm^{-3}}$. The expected phase transition will have significant implications for the possible existence of quark stars and the possibilities depend on the dynamics of the phase conversion as well as on the time scales involved [1–5]. When the phase diagram of bulk matter exhibits a first-order phase transition, the two phases, associated with a high and a low density value (ρ^H and ρ^L), may coexist in mutual thermodynamic equilibrium and, consequently, when brought into physical contact a mechanically stable interface will develop between them. The associated surface tension γ_T depends on the temperature T; it has its largest magnitude at $T = 0$ approaching zero as T is increased to the critical end point temperature, T_c, where the first-order transition line terminates. The surface tension plays a key role in the phase conversion process and it is related to various characteristic quantities such as the nucleation rate, the critical bubble radius, and the favored scale of the blobs generated by the spinodal instabilities [6,7]. For our present purposes, it is important to note that a small surface tension would facilitate various structures in compact stars, including the presence of mixed phases in a hybrid star [8]. Apart from that, a low surface tension leads to other interesting physical phenomena, such as a crust on quark stars [9] and a new type of star called a strangelet dwarf [10].

Early investigations related to the presence of strange quark matter within compact stellar objects have soon recognized the important role played by the surface tension in the development of Fermion-gas models [11,12]. Using the MIT bag model Berger has shown that this quantity is of central importance in order to determine the eventual presence of strange quark matter in the early universe [13] (see also Refs. [14,15] for other early work related to the evaluation of the surface tension within strange matter).

Unfortunately, despite its central importance, the surface tension of quark matter is still rather poorly known. At vanishing temperatures, some early estimates fall within a wide range, typically $\gamma_0 \approx 10$–$50\,\mathrm{MeV/fm^2}$ [12] and values of $\gamma_0 \approx 30\,\mathrm{MeV/fm^2}$ have been considered for studying the effect of quark matter nucleation on the evolution of proto-neutron stars [16]. In Ref. [17], where the effects from charge screening and structured mixed phases have been taken into account, the authors set $20\,\mathrm{MeV/fm^2}$ as a minimal value and then offer an estimate of $\gamma_0 \approx 35$–$50\,\mathrm{MeV/fm^2}$. A higher value, $\gamma_0 \approx 300\,\mathrm{MeV/fm^2}$, is obtained if one performs a naive dimensional analysis of the minimal interface between a color-flavor locked (CFL) phase and nuclear matter [18].

More recently, the surface tension for two-flavor quark matter was evaluated, in Ref. [19], within the the quark meson model (QM), in the framework of the thin-wall approximation for bubble nucleation. The predicted values cover the 5- to 15-MeV/fm^2 range, depending on the inclusion of vacuum and/or thermal corrections. In principle, this range makes nucleation of quark matter possible during the early post-bounce stage of core-collapse supernovae and it is, thus, a rather important result.

The Nambu–Jona-Lasinio model (NJL) with two and three flavors was subsequently considered in the evaluation of

*marcus@fsc.ufsc.br

γ_T [20] via a geometrical approach introduced by Randrup in Ref. [6]. This method makes it possible to express the surface tension for any subcritical temperature in terms of the free energy density for uniform matter in the unstable density range. In practice, the procedure is rather simple to implement and it provides an estimate for the surface tension that is consistent with the equation of state (EOS) implied by the adopted model, with its specific approximations and parametrizations. The results obtained in Ref. [20] predict that, at zero temperature, $\gamma_0 \approx 7$–$30\ \mathrm{MeV/fm^2}$ depending on the chosen parameters.

Very recently, the Polyakov quark meson model (PQM) with three flavors has been considered [21] in the context of the thin-wall approximation extending the work of Ref. [19] with confinement and strangeness. Depending on the adopted parametrization, the numerical results obtained in Ref. [21] are within the $\gamma_0 \approx 13$–$28\ \mathrm{MeV/fm^2}$ range. The authors have confirmed that the inclusion of the strange sector, which was originally done in Refs. [12,15] and also recently in Ref. [20], does not change appreciably the dynamics of the transition at low temperatures and high chemical potentials as neither does the inclusion of the Polyakov loop. Regarding the possibility of phase conversion taking place, within compact stellar objects, it is important to remark that all these three recent evaluations [19–21] predict values for the surface tension which are low enough so, in principle, the phase conversion phenomenon which refers to the spontaneous nucleation of droplets of quark matter could take place [4]. The fundamental role played by the surface tension in the nucleation process for strange and nonstrange matter, which should also depend on other quantities such as the critical pressure for the nuclear/quark transition, has been discussed in Ref. [4]. At the same time, the low value estimates of Refs. [19–21] favor the appearance of a mixed phase within a hybrid star.

One should also recall that very high magnetic fields can be present in magnetars reaching up to $eB \approx 3$–$30m_\pi^2$ ($B \approx 10^{19}$–$10^{20}G$), or higher, at the core of the star [22]. In many applications this type of compact stellar objects are modeled as a hybrid star which has a core of quark matter surrounded by hadronic matter [23]. At the same time, it is important to note that the CFL-nuclear mixed phase disappears when the surface tension rises above $40\ \mathrm{MeV/fm^2}$ [18]. Therefore, if the surface tension between the two phases is small enough, as predicted by Refs. [19–21], the transition occurs via a mixed phase (Gibbs construction). On the other hand, if γ_T has a high value it occurs at a sharp interface (Maxwell construction) [24]. The question of how the surface tension, along with other important physical quantities, is affected by the presence of high magnetic fields has been addressed by Chakrabarty [25] in one of the seminal works related to the investigation of magnetized quark matter. This analysis, which has been carried out in the framework of the conventional MIT bag model with three flavors, predicts that the surface tension of a quark matter bubble diverges for strong magnetic fields when only the lowest Landau level is populated [25,26]. In Ref. [27], which considers magnetized strangelets, it is discussed how this divergence arises when one extends Berger's result for surface corrections [13] so as to account for magnetic fields.

The value of the surface tension in the presence of high magnetic fields may be an important ingredient for investigations related to quark and hybrid stars. However, this type of evaluation does not seem to have been carried out before within a model which displays dynamical symmetry breaking. We intend to perform such a calculation here by extending the work of Ref. [20] so as to account for the presence of high magnetic fields within the NJL model. In this way, our present application adds to the existing literature by furnishing numerical results for the surface tension between the two phases related with chiral symmetry breaking, apart from illustrating how Randrup's approach [6] can be easily generalized to the case where magnetic fields are present.

The coexistence region associated with the (chiral) first-order transition of strongly interacting magnetized matter has been recently investigated in Ref. [28] which predicts, as one of its main results, that the value of ρ^H oscillates around the $B = 0$ value for $0 < eB \lesssim 6m_\pi^2$ and then grows for higher values. Taking into account that γ_T depends on the difference between ρ^H and ρ^L [6,7], one may then expect to find a similar behavior here. Indeed, as we will demonstrate, when a magnetic field is present the surface tension value oscillates very mildly for $0 < eB \lesssim 4m_\pi^2$ before decreasing in a significant way between $4m_\pi^2 \lesssim eB \lesssim 8m_\pi^2$. Then, after reaching a minimum at $eB \approx 5.5m_\pi^2$, it starts to increase, reaching the $B = 0$ value at $eB \approx 9m_\pi^2$, which allows us to conclude that the existence of a mixed phase remains possible within this range of magnetic fields. For eB values higher than $\approx 10m_\pi^2$ this quantity increases rapidly with the magnetic field disfavoring the presence of a mixed phase within hybrid stars. We also show how the temperature affects $\gamma_T(B)$ by decreasing its value towards zero, which is achieved at $T = T_c$, as already emphasized.

The paper is organized as follows. In the next section we review the method for extracting the surface tension from the equation of state (EOS). In Sec. III we present the EOS for the magnetized two-flavor NJL. Then, in Sec. IV, we present our numerical results. The conclusions and final remarks are presented in Sec. V.

II. THE GEOMETRIC APPROACH TO THE SURFACE TENSION EVALUATION

To make this work self-contained let us review, in this section, the geometric approach to the surface tension evaluation which was originally proposed in Ref. [6]. We first assume that the material at hand, strongly interacting matter, may appear in two different phases under the same thermodynamic conditions of temperature T, chemical potential μ, and pressure P. These two coexisting phases have different values of other relevant quantities, such as the energy density $\mathcal{E}$, the net quark number density ρ, and the entropy density s. Under such circumstances, the two phases will develop a mechanically stable interface if placed in physical contact. An interface tension, γ_T, is then associated to this interface.

The two-phase feature appears for all temperatures below the critical value, T_c. Thus, for any subcritical temperature, $T < T_c$, hadronic matter at the density $\rho^L(T)$ has the same chemical potential and pressure as quark matter at the (larger) density $\rho^H(T)$. As T is increased from zero to T_c, the coexistence phase points (ρ^L, T) and (ρ^H, T) trace out the

lower and higher branches of the phase coexistence boundary, respectively, gradually approaching each other and, finally, coinciding for $T = T_c$. Any (ρ, T) phase point outside of this boundary corresponds to thermodynamically stable uniform matter, whereas uniform matter prepared with a density and temperature corresponding to a phase point inside the phase coexistence boundary is thermodynamically unstable and prefers to separate into two coexisting thermodynamically stable phases separated by a mechanically stable interface. Because such a two-phase configuration is in global thermodynamic equilibrium, the local values of T, μ, and P remain unchanged as one moves from the interior of one phase through the interface region and into the interior of the partner phase, as the local density ρ increases steadily from the lower coexistence value ρ^L to the corresponding higher coexistence value ρ^H.

It is convenient to work in the canonical framework where the control parameters are temperature and density. The basic thermodynamic function is, thus, $f_T(\rho)$, the free energy density as a function of the (net) quark number density ρ for the specified temperature T. The chemical potential then can be recovered as $\mu_T(\rho) = \partial_\rho f_T(\rho)$, and the entropy density as $s_T(\rho) = -\partial_T f_T(\rho)$, so the energy density is $\mathcal{E}_T(\rho) = f_T(\rho) - T\partial_T f_T(\rho)$, while the pressure is $P_T(\rho) = \rho\partial_\rho f_T(\rho) - f_T(\rho)$.

For single-phase systems $f_T(\rho)$ is convex, i.e., its second derivative $\partial^2_\rho f_T(\rho)$ is positive, while the appearance of a concavity in $f_T(\rho)$ signals the occurrence of phase coexistence at that temperature. This is easily understood because when $f_T(\rho)$ has a local concave anomaly, then there exist a pair of densities, ρ^L and ρ^H, for which the tangents to $f_T(\rho)$ are common. Therefore $f_T(\rho)$ has the same slope at those two densities, so the corresponding chemical potentials are equal, $\mu_T(\rho^L) = \partial_\rho f_T(\rho^L) = \partial_\rho f_T(\rho^H) = \mu_T(\rho^H)$. Furthermore, because a linear extrapolation of $f_T(\rho)$ leads from one of the touching points to the other, the two pressures are also equal, $P_T(\rho^L) = \rho^L\partial_\rho f_T(\rho^L) - f_T(\rho^L) = \rho^H\partial_\rho f_T(\rho^H) - f_T(\rho^H) = P_T(\rho^H)$. Therefore, uniform matter at the density ρ^L has the same temperature, chemical potential, and pressure as uniform matter at the density ρ^H. The common tangent between the two coexistence points corresponds to the familiar Maxwell construction and shall here be denoted as $f^M_T(\rho)$. Obviously, $f_T(\rho)$ and $f^M_T(\rho)$ coincide at the two coexistence densities and, furthermore, $f_T(\rho)$ exceeds $f^M_T(\rho)$ for intermediate densities. Therefore, we have $\Delta f_T(\rho) \equiv f_T(\rho) - f^M_T(\rho) \geqslant 0$.

For a given (subcritical) temperature T, we now consider a configuration in which the two coexisting bulk phases are placed in physical contact along a planar interface. The associated equilibrium profile density is denoted by $\rho_T(z)$ where z denotes the location in the direction normal to the interface. In the diffuse interface region, the corresponding local free energy density, $f_T(z)$, differs from what it would be for the corresponding Maxwell system, i.e., a mathematical mix of the two coexisting bulk phases with the mixing ratio adjusted to yield an average density equal to the local value $\rho(z)$. This local deficit amounts to

$$\delta f_T(z) = f_T(z) - f_i - \frac{f_T(\rho^H) - f_T(\rho^L)}{\rho^H - \rho^L}[\rho_T(z) - \rho_i], \tag{2.1}$$

where ρ_i is either one of the two coexistence densities. The function $\delta f_T(z)$ is smooth and it tends quickly to zero away from the interface where $\rho_T(z)$ rapidly approaches ρ_i and $f_T(z)$ rapidly approaches $f_T(\rho_i)$. The interface tension γ_T is the total deficit in free energy per unit area of planar interface,

$$\gamma_T = \int_{-\infty}^{+\infty} \delta f_T(z)\, dz. \tag{2.2}$$

As discussed in Ref. [6], when a gradient term used to take account of finite-range effects, the tension associated with the interface between the two phases can be expressed without explicit knowledge about the profile functions but exclusively in terms of the equation of state for uniform (albeit unstable) matter,

$$\gamma_T = a\int_{\rho^L(T)}^{\rho^H(T)} [2\mathcal{E}^g \Delta f_T(\rho)]^{1/2}\frac{d\rho}{\rho^g}, \tag{2.3}$$

where ρ^g is a characteristic value of the density and $\mathcal{E}^g$ is a characteristic value of the energy density, while the parameter a is an effective interaction range related to the strength of the gradient term, $C = a^2\mathcal{E}^g/(\rho^g)^2$. We choose the characteristic phase point to be in the middle of the coexistence region, $\rho^g = \rho_c$ and $\mathcal{E}^g = [\mathcal{E}_0(\rho_c) + \mathcal{E}_c]/2$, where $\mathcal{E}_0(\rho_c)$ is energy density at $(\rho_c, T = 0)$, while $\mathcal{E}_c$ is energy density at the critical point (ρ_c, T_c). The length a is a somewhat adjustable parameter governing the width of the interface region and the magnitude of the tension [6]. In Ref. [20] this parameter was set to $a \approx 1/m_\sigma \approx 0.33$ fm, which also is approximately the value found in an application of the Thomas-Fermi approximation to the NJL model [29]. Therefore, we shall adopt the value $a = 0.33$ fm throughout the present work. With these parameters fixed (see Ref. [20]), the interface tension can be calculated once the free energy density $f_T(\rho)$ is known for uniform matter in the unstable phase region, $\rho^L(T) \leqslant \rho \leqslant \rho^H(T)$.

III. THE EOS FOR THE MAGNETIZED TWO FLAVOR NJL QUARK MODEL

The NJL model is described by a Lagrangian density for fermionic fields given by [30]

$$\mathcal{L}_{\rm NJL} = \bar\psi(i\partial\!\!\!/ - m)\psi + G[(\bar\psi\psi)^2 - (\bar\psi\gamma_5\vec\tau\psi)^2], \tag{3.1}$$

where ψ (a sum over flavors and color degrees of freedom is implicit) represents a flavor iso-doublet (u and d types of quarks) N_c-plet quark fields, while $\vec\tau$ are isospin Pauli matrices. The Lagrangian density (3.1) is invariant under (global) $\mathrm{U(2)_f} \times \mathrm{SU}(N_c)$ and, when $m = 0$, the theory is also invariant under chiral $\mathrm{SU(2)}_L \times \mathrm{SU(2)}_R$. Within the NJL model a sharp cutoff (Λ) is generally used as an ultraviolet regulator and since the model is nonrenormalizable, one has to fix Λ to a value related to the physical spectrum under investigation. This strategy turns the $3+1$ NJL model into an effective model, where Λ is treated as a parameter. The phenomenological values of quantities such as the pion mass (m_π), the pion decay constant (f_π), and the quark condensate ($\langle\bar\psi\psi\rangle$) then are used to fix G, Λ, and m. Here, we choose the set $\Lambda = 590$ MeV and $G\Lambda^2 = 2.435$ with $m = 6$ MeV in order to reproduce $f_\pi = 92.6$ MeV, $m_\pi = 140.2$ MeV, and $\langle\bar\psi\psi\rangle^{1/3} =$

−241.5 MeV [31]. In the MFA the NJL thermodynamic potential can be written as follows [32,33] (see Ref. [34] for results beyond MFA):

$$\Omega^{\rm NJL} = \frac{(M-m)^2}{4G} + \frac{i}{2}{\rm tr}\int \frac{d^4p}{(2\pi)^4}\ln[-p^2+M^2], \quad (3.2)$$

where M is the constituent quarks mass. In order to study the effect of a magnetic field in the chiral transition at finite temperature and chemical potential a dimensional reduction is induced via the following replacements in Eq. (3.2) [35]:

$$\begin{aligned} p_0 &\to i(\omega_\nu - i\mu), \\ p^2 &\to p_z^2 + (2n+1-s)|q_f|B, \\ &\quad \text{with} \quad s=\pm 1, \quad n=0,1,2\ldots, \\ \int_{-\infty}^{+\infty}\frac{d^4p}{(2\pi)^4} &\to i\frac{T|q_f|B}{2\pi}\sum_{\nu=-\infty}^{\infty}\sum_{n=0}^{\infty}\int_{-\infty}^{+\infty}\frac{dp_z}{2\pi}, \end{aligned}$$

where $\omega_\nu = (2\nu+1)\pi T$, where $\nu = 0, \pm1, \pm2\ldots$ represents the Matsubara frequencies for fermions, n represents the Landau levels, and $|q_f|$ is the absolute value of the quark electric charge ($|q_u| = 2e/3$, $|q_d| = e/3$ with $e = 1/\sqrt{137}$ representing the electron charge).[1] Note also that here we have taken the chemical equilibrium condition by setting $\mu_u = \mu_d = \mu$. Then, following Ref. [33], we can write the thermodynamic potential as

$$\Omega^{\rm NJL} = \frac{(M-m)^2}{4G} + \Omega^{\rm NJL}_{\rm vac} + \Omega^{\rm NJL}_{\rm mag} + \Omega^{\rm NJL}_{\rm med}, \quad (3.3)$$

where

$$\Omega^{\rm NJL}_{\rm vac} = -2N_cN_f\int\frac{d^3\mathbf{p}}{(2\pi)^3}(\mathbf{p}^2+M^2)^{1/2}. \quad (3.4)$$

This divergent integral is regularized by a sharp cutoff, Λ, yielding

$$\Omega^{\rm NJL}_{\rm vac} = \frac{N_cN_f}{8\pi^2}\left\{M^4\ln\left[\frac{(\Lambda+\epsilon_\Lambda)}{M}\right] - \epsilon_\Lambda\,\Lambda\left[\Lambda^2+\epsilon_\Lambda^2\right]\right\}, \quad (3.5)$$

where we have defined $\epsilon_\Lambda = \sqrt{\Lambda^2+M^2}$. The magnetic and the in-medium terms are, respectively, given by

$$\begin{aligned} \Omega^{\rm NJL}_{\rm mag} = -\frac{N_c}{2\pi^2}\sum_{f=u}^{d}(|q_f|B)^2\Bigg\{&\zeta^{(1,0)}(-1,x_f) \\ &-\frac{1}{2}\left[x_f^2-x_f\right]\ln(x_f)+\frac{x_f^2}{4}\Bigg\} \end{aligned} \quad (3.6)$$

and

$$\begin{aligned} \Omega^{\rm NJL}_{\rm med} = -\frac{N_c}{2\pi}\sum_{f=u}^{d}\sum_{k=0}^{\infty}\alpha_k|q_f|B \\ \times\int_{-\infty}^{+\infty}\frac{dp_z}{2\pi}\{T\ln[1+e^{-[E_{p,k}(B)+\mu]/T}] \\ +T\ln[1+e^{-[E_{p,k}(B)-\mu]/T}]\}. \end{aligned} \quad (3.7)$$

In the last equation we have replaced the label n by k in the Landau levels in order to account for the degeneracy factor $\alpha_k = 2-\delta_{0k}$. Also, in Eq (3.6) we have used $x_f = M^2/(2|q_f|B)$ and $\zeta^{(1,0)}(-1,x_f) = d\zeta(z,x_f)/dz|_{z=-1}$ with $\zeta(z,x_f)$ representing the Riemann-Hurwitz function (the details of the manipulations leading to the equations above can be found in the appendix of Ref. [33]). Finally, in Eq. (3.7) we have $E_{p,k}(B) = \sqrt{p_z^2+2k|q_f|B+M^2}$, where M is the effective self-consistent quark mass

$$\begin{aligned} M = m + \frac{N_cN_fMG}{\pi^2}\left\{\Lambda\sqrt{\Lambda^2+M^2} - \frac{M^2}{2}\ln\left[\frac{(\Lambda+\sqrt{\Lambda^2+M^2})^2}{M^2}\right]\right\} \\ + \frac{N_cMG}{\pi^2}\sum_{f=u}^{d}|q_f|B\left\{\ln[\Gamma(x_f)] - \frac{1}{2}\ln(2\pi) + x_f - \frac{1}{2}(2x_f-1)\ln(x_f)\right\} \\ - \frac{N_cMG}{2\pi^2}\sum_{f=u}^{d}\sum_{k=0}^{\infty}\alpha_k|q_f|B\int_{-\infty}^{\infty}\frac{dp_z}{E_{p,k}(B)}\left\{\frac{1}{e^{[E_{p,k}(B)+\mu]/T}+1} + \frac{1}{e^{[E_{p,k}(B)-\mu]/T}+1}\right\}. \end{aligned} \quad (3.8)$$

Note that, in principle, one should have two coupled gap equations for the two distinct flavors: $M_u = m_u - 2G(\langle\bar{u}u\rangle + \langle\bar{d}d\rangle)$ and $M_d = m_d - 2G(\langle\bar{d}d\rangle + \langle\bar{u}u\rangle)$, where $\langle\bar{u}u\rangle$ and $\langle\bar{d}d\rangle$ represent the quark condensates which differ, due to the different electric charges. However, in the two-flavor case, the different condensates contribute to M_u and M_d in a symmetric way and since $m_u = m_d = m$ one has $M_u = M_d = M$.

The minimum value of the grand potential represents minus the equilibrium pressure, $\Omega_{\rm min}(T,\mu) = -P$, so the net quark number density is given by $\rho = (\partial P/\partial\mu)_T$. The entropy density given by $s = (\partial P/\partial T)_\mu$, while the energy density, $\mathcal{E}$, can then be obtained by means of the standard thermodynamic relation $P = Ts - \mathcal{E} + \mu\rho$. The knowledge of all these quantities allow us to determine the free energy density, $f \equiv \mathcal{E} - Ts = \mu\rho - P$, as well as the numerical inputs ρ^H, ρ^L, ρ^g, and ϵ^g, which are needed in the evaluation of the surface tension. As already emphasized, the numerical value for the length scale a is chosen to be $1/m_\sigma \simeq 0.33$ fm

[1] We use Gaussian natural units where 1 MeV$^2 = 1.44\times10^{13}\,G$, which sets $m_\pi^2/e \simeq 3\times10^{18}G$.

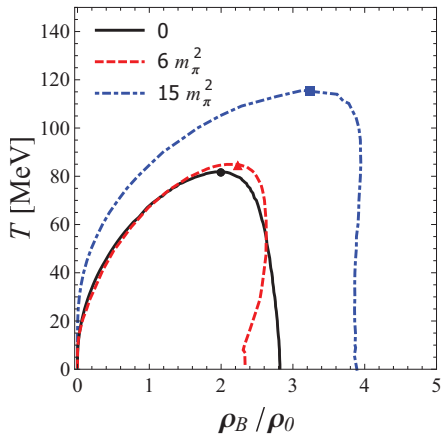

FIG. 1. (Color online) Phase coexistence boundaries in the T-ρ_B plane (ρ_B appears in units of the nuclear matter density, $\rho_0 = 0.17$ fm^{-3}). The solid symbols indicate the location of the critical point for each value of B which occur at ($T_c = 81.1$ MeV, $\mu_c = 324.7$ MeV) for $B = 0$ ($T_c = 84.9$ MeV, $\mu_c = 314.4$ MeV) for $eB = 6m_\pi^2$ and ($T_c = 115.8$ MeV, $\mu_c = 279$ MeV) for $eB = 15m_\pi^2$. Taken from Ref. [28].

(which is about the value found in a Thomas-Fermi application to the NJL model [29]).

IV. NUMERICAL RESULTS

Let us start the numerical evaluations by obtaining the phase diagram in the T-ρ_B plane in order to determine the values of essential quantities such as T_c, μ_c, ρ^H, and ρ^L which allow for the evaluation of the inputs ρ^g and $\mathcal{E}^g$ for each value of B. As is well known, for a given subcritical temperature in the T-ρ_B plane one observes that the associated density region is bounded by the two coexistence densities ρ^L and ρ^H, for which the chemical potential μ has the same value, as does the pressure P. As the density ρ is increased through the lower mechanically metastable (nucleation) region, μ and P rise steadily until the lower spinodal boundary has been reached. Then, as ρ moves through the mechanically unstable (spinodal) region, both μ and P decrease until the higher spinodal boundary is reached. They then increase again as ρ moves through the higher mechanically metastable (bubble-formation) region, until they finally regain their original values at $\rho = \rho^H$. Figure 1 displays the coexistence region, in the T-ρ_B plane, for $B = 0$, $eB = 6m_\pi^2$, and $eB = 15m_\pi^2$. Noting that ρ^H oscillates around the $B = 0$ value and recalling that γ_T depends on the difference between ρ^L and ρ^H, see Eq. (2.3), one can then expect that the surface tension value at $eB = 6m_\pi^2$ will be smaller than at $B = 0$, at least for small temperatures. On the contrary, for $eB = 15m_\pi^2$, one may expect γ_T to assume values much larger than those obtained in the $B = 0$ case. These expectations will be explicitly confirmed by our evaluation of γ_T.

A. The zero-temperature case

In order to illustrate how the method works and also to understand the type of oscillation displayed by Fig. 1 it is convenient to concentrate in the $T = 0$ limit since, in this case, the momentum integrals appearing in the thermodynamical potential can be performed producing equations which are easy to be analyzed from an analytical point of view. Apart from that, this limit is very often considered in evaluations of the EOS for cold stars and it will be our starting point here. Then, in the next subsection, we will analyze how the surface tension is influenced by thermal effects. At $T = 0$ (and also at any other subcritical temperature) the grand potential can present multiple extrema representing stable, metastable, and spinodally unstable matter in the neighborhood of the phase coexistence chemical potential and, as emphasized in Ref. [20], the extraction of the surface tension by the geometric approach requires the consideration of all these extrema. In our case it is then important to know all the gap equation solutions as displayed in Fig. 2 which shows the effective quark mass, at $T = 0$, for $B = 0$, $eB = 6m_\pi^2$, and $eB = 15m_\pi^2$. This effective mass is then used to determine the pressure from where all the other thermodynamic quantities, including the density, can be derived. In this figure, the continuous lines represent the stable solutions only and determine the Maxwell line which links the high effective mass value (M^H) to its low value

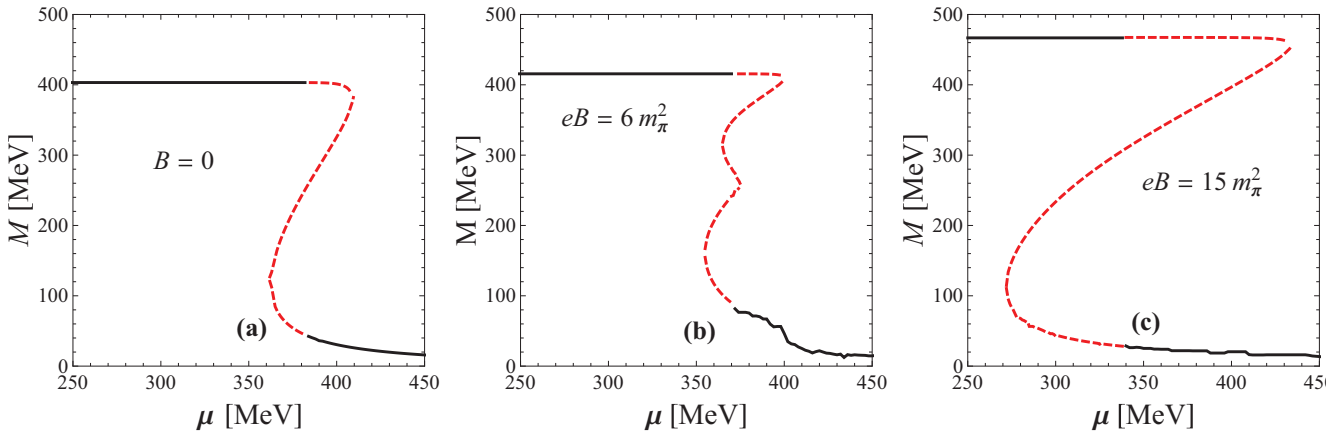

FIG. 2. (Color online) The effective quark mass, at $T = 0$, as a function of μ for $B = 0$ (left panel), $eB = 6m_\pi^2$ (center panel), and $eB = 15m_\pi^2$ (right panel). The continuous lines indicate the gap equation stable solutions and the dashed lines the unstable and metastable ones.

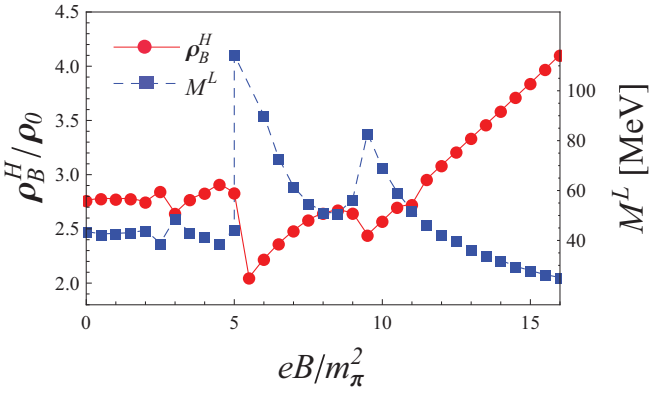

FIG. 3. (Color online) The NJL model effective quark mass (squares) at the lowest value occurring at the transition, M^L, and the highest coexisting baryon density (dots), ρ_B^H (in units of ρ_0), as functions of eB/m_π^2 at $T = 0$. The lines are shown just in order to guide the eye. Taken from Ref. [28].

(M^L) at the coexistence chemical potential where the phase transition occurs. With these two stable solutions and upon using the Maxwell construction one obtains f_T^M. The dashed lines are obtained by considering the unstable as well as the metastable gap equation solutions which lie within the spinodal region. Considering all the gap equation solutions, one then obtains $f_T(\rho)$ to determine the difference $\Delta f_T(\rho)$ which is the crucial ingredient in the surface tension evaluation. But before carrying out the evaluation let us discuss the origin of the de Hass–van Alphen oscillations, for ρ^H, which appear in Fig. 1 at $B \neq 0$. Note from Fig. 2 that, at the coexistence chemical potential, the gap equation for $eB = 6m_\pi^2$, where the oscillations are more pronounced, presents more solutions than the case $B = 0$ or the case $eB = 15m_\pi^2$. The effective mass behavior displayed in Fig. 2 then allows us to understand the ρ^H oscillations, shown in Fig. 1, by reviewing the discussion carried out in Ref. [28]. There it is shown that the decrease in ρ^H for $eB = 6m_\pi^2$, at low temperatures, can be understood in terms of the filling of the Landau levels. With this aim, we present Fig. 3 which displays the baryonic density and the effective quark mass as functions of the magnetic field at $T = 0$. To analyze the figure, let us recall that, in the limit $T \to 0$, the baryonic density can be written[2] as [33]

$$\rho_B(\mu, B) = \theta\left(k_F^2\right) \sum_{f=u}^{d} \sum_{k=0}^{k_{f,\max}} \alpha_k \frac{|q_f| B N_c}{6\pi^2} k_F, \qquad (4.1)$$

where $k_F = \sqrt{\mu^2 - 2|q_f|kB - M^2}$ and

$$k_{f,\max} = \frac{\mu^2 - M^2}{2|q_f|B}, \qquad (4.2)$$

or the nearest integer. Equation (4.1) shows that if $k_F^2 < 0$, then $\rho_B = 0$ which is precisely the low density value at $T = 0$, which is easy to understand by recalling that the effective mass is double valued when the first-order transition occurs presenting a high (M^H) and a low (M^L) value with $M^L < M^H$ for $T < T_c$ and $M^L = M^H$ at $T = T_c$. Now, at $T = 0$, M^H corresponds to the value effective quark mass acquires when $T = 0$ and $\mu = 0$ (the vacuum mass) which corresponds to $M^H \simeq 403$ MeV at $B = 0$, $M^H \simeq 416$ MeV at $eB = 6m_\pi^2$, and $M^H \simeq 467$ MeV at $eB = 15m_\pi^2$. On the other hand, at $T = 0$ the first-order transition happens when $\mu \simeq 383$ MeV for $B = 0$, $\mu \simeq 370$ MeV for $eB = 6m_\pi^2$ and $\mu \simeq 339$ MeV for $eB = 15\,m_\pi^2$ so $\rho^L = 0$ even at the lowest Landau level (LLL), as required by $\theta(k_F^2)$ in Eq. (4.1). Then, to understand the oscillations, let us concentrate on the ρ^H branch, which is shown, together with M^L (the in-medium mass), in Fig. 3, where it is clear that both quantities have an opposite oscillatory behavior. The origin of the oscillations in these quantities can be traced back to the fact that $k_{\max}$ (the upper Landau level filled) decreases as the magnetic field increases. The first and second peaks of the M^L curve correspond to the change from $k_{\max} = 1$ to $k_{\max} = 0$ for the *up*- and *down*-quarks, respectively. For very low temperatures the value of μ at coexistence decreases with B so, generally, $k_{\max}$ and M must vary and when $k_{\max}$ decreases, M increases [28]. It then follows, from Eq. (4.1), that ρ_B must decrease. When $k_{\max} = 0$ for both quark flavors there are no further changes in the upper Landau level and the low temperature oscillations stop at $eB \gtrsim 9.5m_\pi^2$. Note that Eq. (2.3) reveals that the integral defining the surface tension has ρ^H as its upper limit so, intuitively, one could expect that, in principle, γ_T will also oscillate following a pattern similar to the one shown in Fig. 3 for ρ^H.

Let us now obtain the surface tension at vanishing temperature by first obtaining the difference $\Delta f_0(\rho) \equiv f_0(\rho) - f_0^M(\rho)$. Since $f_T(\rho) = \rho\mu(\rho) - P_T(\rho)$ one can start by evaluating $\mu(\rho)$ and $P(\rho)$ for uniform matter within the thermodynamically unstable region of the phase diagram. Figures 4 and 5 show the results for $\mu(\rho)$ and $P(\rho)$ respectively and, as before, the continuous lines reflect the stable gap equation solutions and the dashed lines the unstable and metastable ones. It is then an easy task to obtain a (positive) deviation, $\Delta f_0(\rho)$, which determines the surface tension. Figure 6 shows $\Delta f_0(\rho)$ for $B = 0$, $eB = 6m_\pi^2$, and $eB = 15m_\pi^2$ displaying the expected oscillatory behavior around the $B = 0$ case. Figure 7, which constitutes our main result, shows the surface tension as a function of eB at $T = 0$, showing that it oscillates around the $B = 0$ value for $0 < eB \lesssim 4m_\pi^2$ before decreasing about 30% for $4m_\pi^2 \lesssim eB \lesssim 8m_\pi^2$. Then, after reaching a minimum at $eB \approx 5.5m_\pi^2$, it starts to increase again, reaching the $B = 0$ value at $eB \approx 9m_\pi^2$. After that, only the LLL is filled and γ_0 continues to grow with B. This behavior can be roughly explained by recalling that the surface tension, as given by Eq. (2.3), is proportional to the area determined by $\Delta f_0(\rho)$ as shown in Fig. 6. Since this area depends on the upper limit (ρ^H) of the integral representing γ_T the pattern observed in Fig. 7 can be further understood by comparing this figure with Fig. 3, which shows ρ^H as a function of eB. As one can see, both γ_0 (in Fig. 7) and ρ^H (in Fig. 3) approximately behave in the same way, which is just the opposite behavior of M^L (also shown in Fig. 3). As we have already discussed, for low values of the magnetic field M^L oscillates as consequence of the filling of Landau levels but the oscillations stop when

[2]There is a misprint in Eq. (30) of Ref. [33] where it should be ρ_B instead of ρ.

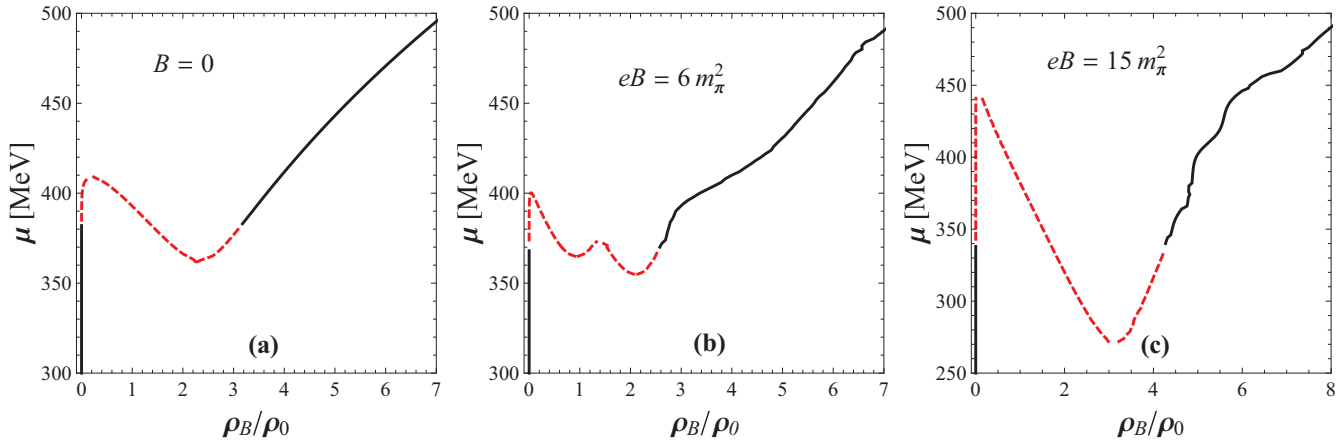

FIG. 4. (Color online) The chemical potential as a function of ρ_B/ρ_0 for $B = 0$, $eB = 6m_\pi^2$, and $eB = 15m_\pi^2$. The continuous lines indicate the gap equation stable solutions and the dashed lines the unstable and metastable ones.

only the LLL is available for both flavors, which, in our case, happens at $eB \gtrsim 9.5m_\pi^2$. From this value onwards M^L decreases with B while ρ^H increases, as Eq. (4.1) shows, so γ_0 also increases, as observed in Fig. 7. The abrupt decrease of γ_0 (and ρ^H) at $eB \approx 5.5m_\pi^2$, which could also be expected, is a result of the sudden increase of M^L, with the consequent abrupt decrease of ρ^H, when $k_{\max}$ for the up-quark changes from $k_{\max} = 1$ to $k_{\max} = 0$. In summary, the surface tension behavior observed in Fig. 7 could be anticipated from the behavior of ρ^H and M^L shown in Fig. 3, since these quantities are related via Eqs. (2.3) and (4.1). Of course, the behaviors of ρ^H and γ_T are very similar but not identical because the latter quantity also depends on $\Delta f_T(\rho)$, $\mathcal{E}^g$, and ρ^g. Note that other physical quantities, such as the latent heat, which also depends on the difference between the high and the low densities, oscillate in a similar way [28]. We refer the interested reader to Ref. [36], where the oscillations associated with this type of model have been discussed in great detail.

Finally, Table I summarizes all our results for γ_0, when $B = 0$, $eB = 6m_\pi^2$, and $eB = 15\,m_\pi^2$, and also lists the characteristic values $\mathcal{E}^g$ and ρ^g as well as the location of the critical point (T_c, μ_c) and the upper integral limit [see Eq. (2.3)], ρ^H. For the present model approximation, $\rho^L = 0$ in all cases. The table also shows that the values of the constituent quark mass, at $T = 0$ and $\mu = 0$, grow with B in accordance with the magnetic catalysis phenomenon.

B. Thermal effects

Let us now investigate how thermal effects influence the interface tension since this quantity is expected to decrease with increasing temperature because both the coexistence densities and the associated free energy densities move closer together at higher T; they ultimately coincide at T_c, where, therefore, the tension vanishes. This general behavior is confirmed by our calculations, as shown in Fig. 8. The temperature dependence of the surface tension may be relevant for the thermal formation of quark droplets in cold hadronic matter found in "hot" protoneutron stars whose temperatures, T_*, are of the order 10–20 MeV [4,14,37,38]. The temperature

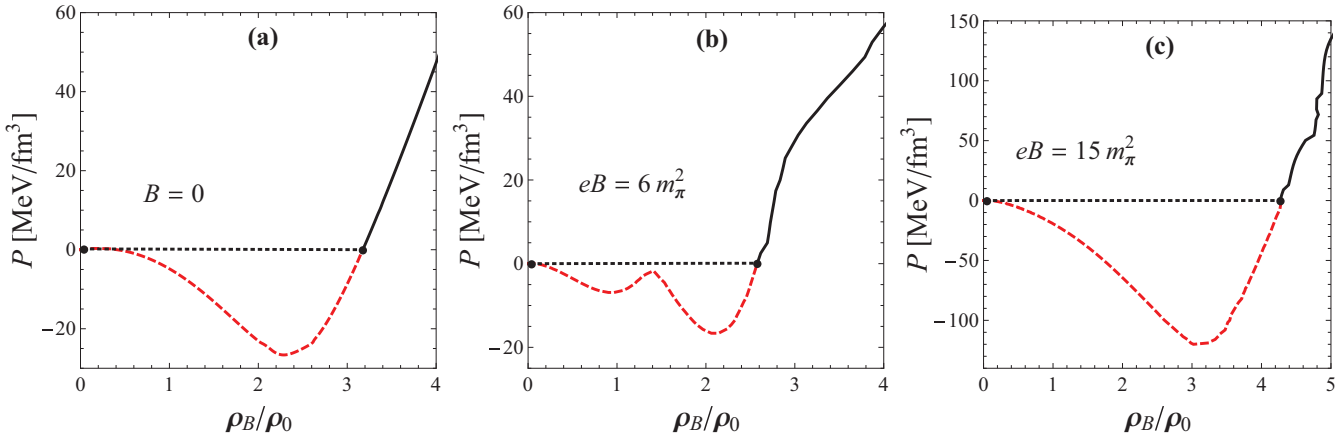

FIG. 5. (Color online) The pressure as a function of ρ_B/ρ_0 for $B = 0$, $eB = 6m_\pi^2$, and $eB = 15m_\pi^2$. The continuous lines indicate the gap equation stable solutions and the dashed lines the unstable and metastable ones. The dotted lines joining the solid dots represent the Maxwell construction.

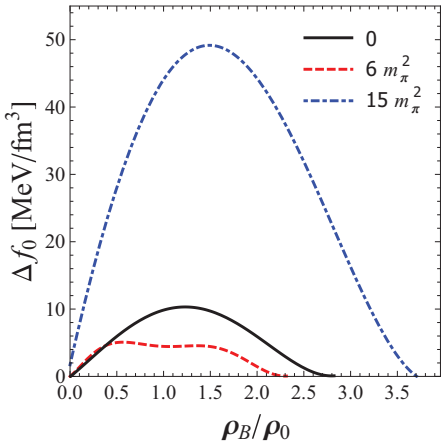

FIG. 6. (Color online) The quantity Δf_0 as a function of ρ_B/ρ_0 for $B = 0$, $eB = 6m_\pi^2$, and $eB = 15m_\pi^2$.

dependence of the surface tension is also important in the context of heavy-ion collisions, because it determines the favored size of the clumping caused by the action of spinodal instabilities as the expanding matter traverses the unstable phase-coexistence region [6].

C. Other possible effects

So far, our results for the surface tension were obtained within a certain model approximation, namely the standard two-flavor NJL model at the mean-field level. Therefore, one may wonder how other possibilities, including a different parametrization, strangeness, vector interactions, corrections beyond the MFA, and confinement, among others, would eventually influence our numerical predictions. Let us start this discussion with the parametrization issue, in which case it becomes important to recall that, within the NJL model, a stronger coupling increases the first-order transition line in the T-μ plane. This fact is reflected by an increase of the coexistence region in the T-ρ_B plane. Then, a stronger coupling should produce a higher surface tension, which is indeed the case, as demonstrated in Ref. [20] for $B = 0$. For example, taking $\Lambda = 631$ MeV, $G\Lambda^2 = 2.19$, and $m = 5.5$ MeV the critical point occurs at $T_c = 46$ MeV and $\mu_c = 332$ MeV while the effective quark mass value is $M = 337$ MeV (compare with our values in Table I). With this parametrization, one obtains $\gamma_0 = 7.11$ MeV/fm^2, which is much smaller than our value, $\gamma_0 = 30.38$ MeV/fm^2. On the other hand, the surface tension value is expected to increase by taking a higher coupling but one should also remember that the effective quark mass grows with G and, with the set adopted here, we already have $M = 403$ MeV, which can be considered high enough.[3] Therefore, as far as the parametrization is concerned, our predictions could be lowered by adopting coupling values which predict smaller values for the effective quark mass.

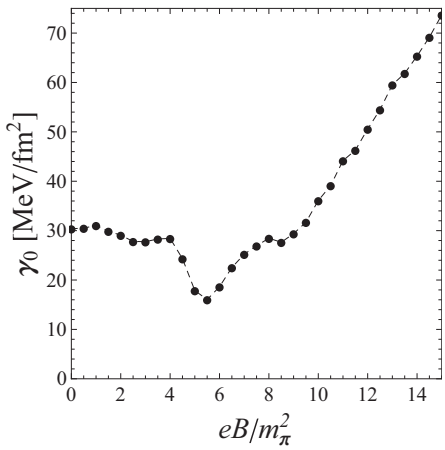

FIG. 7. The surface tension at vanishing temperature, γ_0, as a function of eB (in units of m_π^2). The lines are shown just in order to guide the eye.

TABLE I. Summary of inputs and results at $T = 0$ for different values of eB (in units of m_π^2). The length parameter was taken as $a = 0.33$ fm. The characteristic energy density $\mathcal{E}^g$ is given in MeV/fm^3, and the critical values μ_c and T_c are given in MeV. The effective magnetic quark masses M (at $\mu = 0$) are also given in MeV while the resulting zero-temperature surface tension γ_0 is given in MeV/fm^2. In all cases $\rho_B^L = 0$ and $\rho_0 = 0.17$/fm^3.

eB	γ_0	M	T_c	μ_c	ρ_B^H/ρ_0	ρ_B^g/ρ_0	$\mathcal{E}^g$
0	30.38	403	81.1	324.7	2.73	2.03	495
6	18.63	416	84.9	314.4	2.2	2.17	476
15	73.68	467	115.8	279.0	3.8	3.17	705

Next, let us point out that the presence of a repulsive vector channel may play an important role when treating the NJL at finite densities and, in this case, an interaction of the form $-G_V(\bar{\psi}\gamma^\mu\psi)^2$ is usually added to the Lagrangian density describing the model [32,39]. Then, regarding the phase diagram, it has been established that the net effect of a repulsive vector contribution, parametrized by the coupling G_V, is to add a term $-G_V\rho^2$ to the pressure, weakening the first-order transition [40]. In this case, the first-order transition line shrinks, forcing the CP to appear at smaller temperatures, while the first-order transition occurs at higher coexistence chemical potential values as G_V increases. In this case, the coexistence region decreases (this situation will not be affected by the presence of a magnetic field [41]) and should produce an even smaller value for the surface tension.

With respect to the MFA adopted here, we believe that further improvements will only reduce the surface tension since evaluations performed with the nonperturbative optimized perturbation theory (OPT), at $G_V = 0$, have shown [34] that as early as at the first nontrivial order the free energy receives contributions from two loop terms which are $1/N_c$ suppressed. It turns out that these exchange (Fock) type of terms, which do not contribute at the large-N_c (or MFA) level, produce a net effect similar to the one observed with the MFA at $G_V \neq 0$. This is due to the fact that the OPT pressure displays a term of the form $-G_S/(N_f N_c)\rho^2$, where G_S is

[3] In most works the coupling is chosen so M is about one-third of the baryonic mass (≈310 MeV).

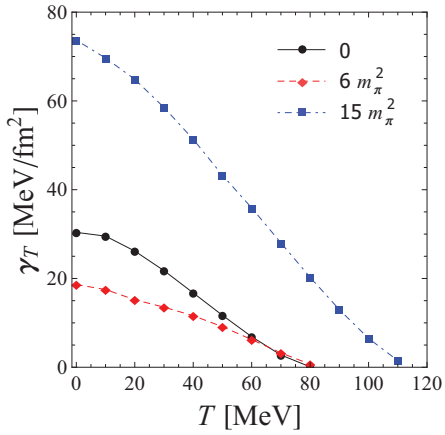

FIG. 8. (Color online) The surface tension, γ_T, as a function of the temperature for $B = 0$, $eB = 6m_\pi^2$, and $eB = 15m_\pi^2$. The lines are shown just in order to guide the eye.

the usual scalar coupling so a vector-like contribution can be generated by quantum corrections, even when $G_V = 0$ at the Lagrangian (tree) level. The relation between the MFA (at $G_V \neq 0$) and the OPT (at $G_V = 0$) and their consequences for the first-order phase transition has been recently analyzed in great detail [42]. Based on this result, one concludes that, in principle, the inclusion of corrections beyond the mean-field level may contribute to further decrease the value of γ_T.

In stellar modeling, the structure of the star depends on the assumed EOS built with appropriate models while the true ground state of matter remains a source of speculation. It has been argued [43] that *strange quark matter* (SQM) is the true ground state of all matter and this hypothesis is known as the Bodmer-Witten conjecture. Hence, the interior of neutron stars should be composed predominantly of u, d, and s quarks (plus leptons if one wants to ensure charge neutrality). The question of how strangeness affects γ_0 was originally addressed in Refs. [12,15] within a Fermion-gas model and the MIT bag model, respectively. The three-flavor NJL was considered within Randrup's approach, yielding the value $\gamma_0 = 20.42$ MeV/fm^2, which is still within the lower end of estimated values [20]. Moreover, in their application to the three-flavor Polyakov quark meson model, the authors of Ref. [21] have confirmed that the presence of strangeness should not affect the surface tension in a drastic way. Another important issue, treated in Ref. [21], concerns confinement which has been considered by means of the Polyakov loop. Also, in this case, the main outcome is that the surface tension value is not too much affected when the quark model is extended by the Polyakov loop.

Together, all these remarks indicate that our (low end) estimates for γ_T are basically stable to the inclusion of more refinements (such as strangeness and confinement) and can even be further lowered (e.g., by going beyond the mean-field level and/or by including a repulsive vector channel).

V. CONCLUSIONS

In this work we have evaluated the surface tension related to the first-order chiral phase transition for two-flavor magnetized quark matter by considering the NJL model in the MFA. To obtain this quantity we have used the prescription presented in Ref. [6], which is straightforward once the uniform-matter equation of state is available for the unstable regions of the phase diagram. The surface tension determined in the present fashion is entirely consistent with the employed model, including the approximations and parametrizations adopted. In practice, one only needs to consider *all* the solutions to the gap equation (stable, metastable and unstable) when generating the corresponding EOS. This method was previously employed to obtain the surface tension for the NJL in the absence of magnetic fields yielding $\gamma_0 \lesssim 30$ MeV/fm^2, which lies within the low end of available estimates ($\gamma_0 \approx$ 10–300 MeV/fm^2) and is in agreement with other recent predictions which employ effective quark models [19,21]. The importance of this result concerns, for example, the possibility of a mixed phase occurring in hybrid stars since the existence of such a phase is possible when the surface tension has a low value [23].

Our results have shown that, when a magnetic field is present, the surface tension value presents a small oscillation around the $B = 0$ value for $0 < eB \lesssim 4m_\pi^2$. It then decreases for $4m_\pi^2 \lesssim eB \lesssim 8m_\pi^2$, reaching a minimum at $eB \approx 5.5m_\pi^2$, where the value is about 30% smaller than the $B = 0$ result. After this point it starts to increase continuously, reaching the $B = 0$ value at $eB \approx 9m_\pi^2$. This result allows us to conclude that the existence of a mixed phase remains possible within this range of magnetic fields and can even be favored at the core of magnetars if $B \sim 1.8 \times 10^{19} G$ (or, equivalently, $eB \sim 6m_\pi^2$). At about twice this field intensity the surface tension starts to increase rapidly with the magnetic field disfavoring the presence of a mixed phase within hybrid stars. The origin of this behavior can be traced back to the oscillations present in the coexistence region, which is a quantity of central importance in the evaluation of γ_T. We have also shown how the temperature affects this quantity by decreasing its value towards zero, which is achieved at $T = T_c$, as expected. Other issues, such as strangeness, the presence of a repulsive vector interaction, confinement, corrections to the MFA, as well as different parametrizations, have also been discussed. We have argued that our surface tension values, which already rank at the low end of the available wide range of predictions, will be little affected by strangeness and confinement and will be even lowered by the presence of a repulsive vector term and/or by the inclusion of corrections beyond the mean-field level so a mixed phase within hybrid stars will be further favored by these improvements. On the other hand, with the adopted model, the surface tension value could grow if one chooses a parametrization with a coupling greater than ours, which, in turn, would lead to very high effective quark masses.

ACKNOWLEDGMENTS

A.F.G. thanks Capes for support and M.B.P. thanks CNPq for partial support. This work also received funding from Fundação de Amparo à Pesquisa e Inovação do Estado de Santa Catarina (FAPESC). The authors are grateful to Veronica Dexheimer for her comments and suggestions.

[1] E. S. Fraga, R. D. Pisarski, and J. Schaffner-Bielich, Phys. Rev. D **63**, 121702 (2001); Nucl. Phys. A **702**, 217 (2002).

[2] J. Schaffner-Bielich, J. Phys. G **31**, S651 (2005), and references therein.

[3] I. Sagert *et al*., Phys. Rev. Lett. **102**, 081101 (2009).

[4] B. W. Mintz, E. S. Fraga, G. Pagliara, and J. Schaffner-Bielich, J. Phys. G **37**, 094066 (2010); Phys. Rev. D **81**, 123012 (2010).

[5] I. Bombaci, D. Logoteta, P. K. Panda, C. Providencia, and I. Vidana, Phys. Lett. B **680**, 448 (2009).

[6] J. Randrup, Phys. Rev. C **79**, 054911 (2009).

[7] Ph. Chomaz, M. Colonna, and J. Randrup, Phys. Rep. **389**, 263 (2004).

[8] A. Kurkela, P. Romatschke, A. Vuorinen, and B. Wu, arXiv:1006.4062 [astro-ph.HE].

[9] M. G. Alford and D. A. Eby, Phys. Rev. C **78**, 045802 (2008).

[10] M. G. Alford, S. Han, and S. Reddy, J. Phys. G **39**, 065201 (2012).

[11] E. Farhi and R. L. Jaffe, Phys. Rev. D **30**, 2379 (1984).

[12] M. S. Berger and R. L. Jaffe, Phys. Rev. C **35**, 213 (1987); **44**, 566(E) (1991).

[13] M. S. Berger, Phys. Rev. D **40**, 2128 (1989); **43**, 4150(E) (1991).

[14] M. L. Olesen and J. Madsen, Phys. Rev. D **49**, 2698 (1994).

[15] J. Madsen, Phys. Rev. D **50**, 3328 (1994).

[16] I. Bombaci, D. Logoteta, C. Providencia, and I. Vidana, Astron. Astrophys. **462**, 1017 (2007).

[17] D. N. Voskresensky, M. Yasuhira, and T. Tatsumi, Nucl. Phys. A **723**, 291 (2003).

[18] M. G. Alford, K. Rajagopal, S. Reddy, and F. Wilczek, Phys. Rev. D **64**, 074017 (2001).

[19] L. F. Palhares and E. S. Fraga, Phys. Rev. D **82**, 125018 (2010).

[20] M. B. Pinto, V. Koch, and J. Randrup, Phys. Rev. C **86**, 025203 (2012).

[21] B. W. Mintz, R. Stiele, R. O. Ramos, and J. Schaffner-Bielich, Phys. Rev. D **87**, 036004 (2013).

[22] D. Lai and S. L. Shapiro, Astrophys. J. **383**, 745 (1991); M. Bocquet, S. Bonazzola, E. Gourgoulhon, and J. Novak, Astron. Astrophys. **301**, 757 (1995); S. Chakrabarty, D. Bandyopadhyay, and S. Pal, Phys. Rev. Lett. **78**, 2898 (1997); D. Bandyopadhyay, S. Chakrabarty, and S. Pal, *ibid*. **79**, 2176 (1997); A. E. Broderick, M. Prakash, and J. M. Lattimer, Phys. Lett. B **531**, 167 (2002); F. Weber, M. Meixner, R. P. Negreiros, and M. Malheiro, Int. J. Mod. Phys. E **16**, 1165 (2007); E. J. Ferrer, V. de la Incera, J. P. Keith, I. Portillo, and P. L. Springsteen, Phys. Rev. C **82**, 065802 (2010).

[23] V. Dexheimer, R. Negreiros, and S. Schramm, Eur. Phys. J. A **48**, 189 (2012); J. Phys. Conf. Ser. **432**, 012005 (2013).

[24] M. Alford, S. Han, and M. Prakash, arXiv:1302.4732 [astro-ph.SR].

[25] S. Chakrabarty, Phys. Rev. D **54**, 1306 (1996).

[26] T. Ghosh and S. Chakrabarty, Phys. Rev. D **63**, 043006 (2001).

[27] R. Gonzales Felipe, E. Lopez Fune, D. Manreza Paret, and A. Perez Martinez, J. Phys. G **39**, 045006 (2012).

[28] G. N. Ferrari, A. F. Garcia, and M. B. Pinto, Phys. Rev. D **86**, 096005 (2012).

[29] S. V. Molodtsov and G. M. Zinovjev, Phys. Rev. D **84**, 036011 (2011).

[30] Y. Nambu and G. Jona-Lasinio, Phys. Rev. **122**, 345 (1961); **124**, 246 (1961).

[31] M. Frank, M. Buballa, and M. Oertel, Phys. Lett. B **562**, 221 (2003).

[32] M. Buballa, Phys. Rep. **407**, 205 (2005).

[33] D. P. Menezes, M. B. Pinto, S. S. Avancini, A. P. Martínez, and C. Providência, Phys. Rev. C **79**, 035807 (2009).

[34] J.-L. Kneur, M. B. Pinto, and R. O. Ramos, Phys. Rev. C **81**, 065205 (2010); L. Ferroni, V. Koch, and M. B. Pinto, *ibid*. **82**, 055205 (2010).

[35] E. S. Fraga and A. J. Mizher, Phys. Rev. D **78**, 025016 (2008).

[36] D. Ebert, K. G. Klimenko, M. A. Vdovichenko, and A. S. Vshivtsev, Phys. Rev. D **61**, 025005 (1999).

[37] J. E. Horvath, O. G. Benvenuto, and H. Vucetich, Phys. Rev. D **45**, 3865 (1992).

[38] T. Fischer, S. C. Whitehouse, A. Mezzacappa, F. K. Thielemann, and M. Liebendorfer, Astron. Astrophys. **499**, 1 (2009).

[39] V. Koch, T. S. Biro, J. Kunz, and U. Mosel, Phys. Lett. B **185**, 1 (1987).

[40] K. Fukushima, Phys. Rev. D **77**, 114028 (2008).

[41] R. Z. Denke and M. B. Pinto, arXiv:1306.6246 [hep-ph].

[42] J.-L. Kneur, M. B. Pinto, R. O. Ramos, and E. Staudt, Int. J. Mod. Phys. E **21**, 1250017 (2012).

[43] N. Itoh, Prog. Theor. Phys. **44**, 291 (1970); A. R. Bodmer, Phys. Rev. D **4**, 1601 (1971); E. Witten, *ibid*. **30**, 272 (1984); P. Haensel, J. L. Zdunik, and R. Schaeffer, Astron. Astrophys. **160**, 121 (1986); C. Alcock, E. Farhi, and A. Olinto, Astrophys. J. **310**, 261 (1986).